Inorg. Chem. **2004**, *43*, 6408–6413

Charge-Transfer Hybrids Containing Covalently Bonded Polyoxometalates and Ferrocenyl Units

Jeonghee Kang,[†] James A. Nelson,[†] Meng Lu,[†] Baohan Xie,[†] Zhonghua Peng,*[,†] and Douglas R. Powell[‡]

Departments of Chemistry, University of Missouri−Kansas City, Kansas City, Missouri 64110, and University of Kansas, Lawrence, Kansas 66045

Received June 9, 2004

Two new charge-transfer hybrids with one or two ferrocenyl units covalently attached to a hexamolybdate cluster through an extended π-conjugated bridge have been prepared using Pd-catalyzed coupling reactions on monoiodo- or diiodo-functionalized cluster substrates in over 60% yields. These hybrids have been characterized by ^{1}H NMR, FTIR, electrospray ionization mass spectrometry, and X-ray diffraction. The electronic spectra of these hybrids show a broad absorption tail extending beyond 550 nm, indicating the existence of charge-transfer transition from the ferrocenyl donor to the cluster acceptor. The observation of the clear charge-transfer transition indicates the contribution of charge-transfer resonance to the ground state in both **2a** and **2b** even though the donor–acceptor separation distance of 11.29 Å is rather long, signaling a through-bond charge-transfer nature made possible by the organic π-conjugated bridge. Cyclic voltammetry studies reveal a one-electron oxidation wave and a one-electron reduction wave for the hybrid with one ferrocenyl unit. For the one with two ferrocenyl units, a lower reduction potential and a two-electron oxidation wave are observed, indicating negligible electronic interactions between the two ferrocenyl units.

Introduction

Charge-transfer hybrids involving organic donors and inorganic acceptors have been the focus of research for many decades.[1] Aside from searching for nonmetal metallic conductors, realizing new materials with cooperative or collective properties such as superconductivity, ferromagnetism, nonlinear optical properties, etc. has been one of the major driving forces.[2] Recent discovery that such hybrids could result in highly efficient photovoltaic cells has further stimulated research on charge transfer through organic−inorganic heterojunctions or interfaces.[3] Polyoxometalates (POMs), early-transition-metal−oxygen anion clusters, are well-known electron acceptors.[4] Not surprisingly, POMs have been widely applied in preparing charge-transfer salts with organic cation donors.[5] Charge-transfer materials based on neutral organic π-donors and POM clusters have also been prepared through cocrystallization.[6,7] Nearly all of these POM-containing hybrids, however, bring the organic and the inorganic components together through Coulombic interactions. Covalently bonded charge-transfer molecular hybrids

* Author to whom correspondence should be addressed. E-mail: pengz@umkc.edu.

[†] University of Missouri−Kansas City.

[‡] University of Kansas.

(1) (a) Sakata, T.; Hashimoto, K.; Hiramoto, M. *J. Phys. Chem.* **1990**, *94*, 3040. (b) Tatada, J.; Awaji, H.; Koshioka, M.; Nakajima, A.; Nevin, W. A. *Appl. Phys. Lett.* **1992**, *61*, 2184. (c) Miyasaka, T.; Watanabe, T.; Fujishima, A.; Honda, K. *J. Am. Chem. Soc.* **1978**, *100*, 6657. (d) SakaOzin, G. A. *Adv. Mater*. **1992**, *4*, 612. (e) Jundeinstein, P.; Sanchez, C. *J. Mater. Chem.* **1996**, *6*, 511. (f) Okabe, A.; Fukushima, T.; Ariga, K,; Aida, T. *Angew. Chem., Int. Ed.* **2002**, *41*, 3414. (g) Bose, A.; He, P.; Liu, C.; Ellman, B. D.; Twieg, R. J.; Huang, S. D. *J. Am. Chem. Soc.* **2002**, *1*, 4.

(2) (a) Lacroix, P. G. *Chem. Mater*. **2001**, *13*, 3495−3506. (b) Mitzi, D. B. *Chem. Mater*. **2001**, *13*, 3283−3298 and references therein. (c) Ishiguro, T.; Yamaji, K.; Saito, G. *Organic Superconductors*; Springer-Verlag: Berlin, 1998. (d) Itoh, K.; Kinoshita, M. *Molecular Magnetism: New Magnetic Materials*; Dodansha and Gordon & Breach: Tokyo and Amsterdam, 2001. (e) Mitzi, D. B. *Prog. Inorg. Chem.* **1999**, *48*, 1.

(3) (a) Huynh, W. U.; Dittmer, J. J.; Alivisatos, A. P. *Science* **2002**, *295*, 2425. (b) Sun, B.; Marx, E.; Greenham, N. C. *Nano Lett.* **2003**, *3*, 961. Liu, J. S.; Tanaka, T.; Sivula, K.; Alivisatos, A. P.; Fréchet, J. M. J. *J. Am. Chem. Soc.* **2004**,

(4) (a) Sadakane, M.; Steckhan, E. *Chem. Rev.* **1998**, *98*, 219. (b) Yamase, T. *Chem. Rev.* **1998**, *98*, 307. (c) Pope, M. T. *Prog. Inorg. Chem.* **1991**, *30*, 181.

(5) (a) Torres, G. R.; Dupart, E.; Mingotaud, C.; Ravaine, S. *J. Phys. Chem. B* **2000**, *104*, 9487. (b) Liu, S.; Kurth, D. G.; Bredenkötter, Volkmer, D. *J. Am. Chem. Soc.* **2002**, *124*, 12279. (c) Wang, X.; Gauo, Y.; Li, Y.; Wang, E.; Hu, C.; Hu, N. *Inorg. Chem.* **2003**, *42*, 4135. (d) Grigoriev, V. A.; Cheng, D.; Hill, C. L.; Weinstock, I. A. *J. Am. Chem. Soc*. **2001**, *123*, 5292−5307.

(6) Coronado, E.; Gómez-García, C. J. *Chem. Rev.* **1998**, *98*, 273 and references therein.

10.1021/ic049250x CCC: $27.50
Published on Web 09/04/2004

Scheme 1. Synthesis of Charge-Transfer Hybrids **2a** and **2b**[a]

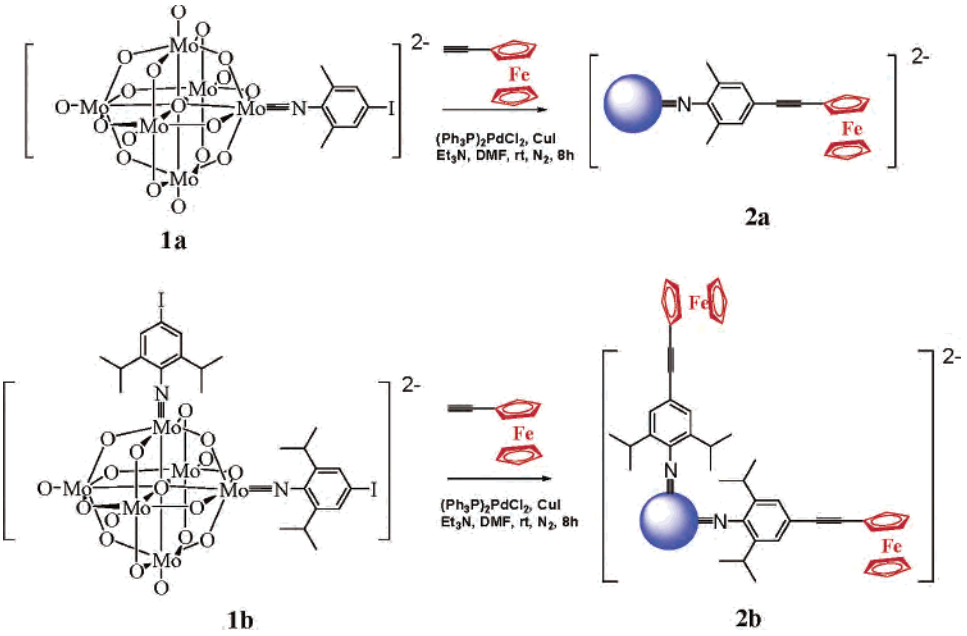

[a] The counterion is tetrabutylammonium.

are still scarce.[8] One pioneering example was reported nearly a decade ago where a ferrocenyl unit was bonded directly to a hexamolybdate cluster through a Mo−N imido bond.[9] This hybrid, which shows an intramolecular charge-transfer transition at 536 nm, was prepared, however, in only 19% yield through a direct functionalization reaction on the hexamolybdate cluster. The short separation distance between the ferrocenyl donor and the cluster acceptor also renders the charge recombination facile as a coherent superexchange mechanism dominates.[10] In this Article, we report two charge-transfer hybrids in which one or two ferrocenyl units are linked to a hexamolybdate cluster through an extended π-conjugated bridge. These hybrids were prepared in high yields using a rational building block approach developed recently in our laboratory.[11] The detailed synthesis, structural characterizations, and physical properties of these new hybrids are presented.

Results and Discussion

Synthesis of Charge-Transfer Hybrids. Scheme 1 shows the synthesis of hybrids **2a** and **2b**. The selective synthesis of monoiodo- or diiodo-functionalized hexamolybdates **1a** and **1b** was reported previously.[12] The Pd-catalyzed Sonogashira coupling of **1a** or **1b** with ethynylferrocene was carried out at room temperature in DMF. As demonstrated previously,[13] the coupling reaction went smoothly and the resulting hybrids were isolated in over 60% yields. Both hybrids are red crystals and soluble in methylene chloride and acetonitrile. However, only **2b** is soluble in chloroform and tetrahydrofuran. Both hybrids are insoluble in ethyl ether. Single crystals of **2a**, suitable for X-ray crystal structure determination, were grown from the slow diffusion of ethyl ether into a methylene chloride solution of **2a**. For **2b**, the same procedure has so far resulted in only multicrystalline solids.

The structures of **2a** and **2b** have been confirmed by ^{1}H NMR studies. As shown in Figure 1, the ^{1}H NMR spectra of **2a** and **2b** show clearly resolved sharp signals which can all be unambiguously assigned. The aryl protons in **2a** and **2b** give a singlet at 7.14 and 7.20 ppm, respectively, while the protons in the cyclopentadienyl (Cp) units show two triplets and one singlet between 4 and 5 ppm. The methyl protons in **2a** give a singlet at 2.58 ppm, while the protons of the isopropyl group in **2b** appear at 1.29 and 3.87 ppm. Signals at 0.95, 1.34, 1.59, and 3.07 ppm are attributed to protons in the tetrabutylammonium counterions. Integration of signals from the counterion such as the one at 3.07 ppm and those from the attached organic segments such as the one at 7.14 or 7.20 ppm confirms the linkage of one and two ferrocenyl units in **2a** and **2b**, respectively, to the cluster.

The FTIR spectrum of **2a** shows one strong band at 794 cm^{-1} and one weak band at 878 cm^{-1}, which are attributed

(7) (a) Hill, C. L.; Bouchard, D. A.; Kadkhodayan, M.; Williamson, M. M.; Schmidt, J. A.; Hilinski, E. F. *J. Am. Chem. Soc.* **1988**, *110*, 5471. (b) Attanasio, D.; Bonamico, M.; Fare, V.; Imperatori, P.; Suber, L. *J. Chem. Soc., Dalton Trans.* **1990**, 3221. (c) Niu, J. Y.; You, X. Z.; Duan, C. Y.; Fun, H. K.; Zhou, Z. Y. *Inorg. Chem.* **1996**, *35*, 4211. (d) Maguerès, P. Le; Hubig, S. M.; Lindeman, S. V.; Veya, P.; Kochi, J. K. *J. Am. Chem. Soc.* **2000**, *122*, 10073.
(8) (a) Gouzerh, P.; Proust, A. *Chem. Rev.* **1998**, *98*, 77. (b) Strong, J. B.; Yap, G. P. A.; Ostrander, R.; Liable-Sands, L. M.; Rheingold, A. L.; Thouvenot, R.; Gouzerh, P.; Maatta, E. A. *J. Am. Chem. Soc.* **2000**, *122*, 639−649. (c) Bar-Nahum, I.; Cohen, H.; Neumann, R. *Inorg. Chem.* **2003**, *42*, 3677.
(9) Stark, J. L.; Young, V. G., Jr.; Maatta, E. A. *Angew. Chem., Int. Ed. Engl.* **1995**, *34*, 2547.
(10) Weiss, E. A.; Ahrens, M. J.; Sinks, L. E.; Gusev, A. V.; Ratner, M. A.; Wasielewski, M. R. *J. Am. Chem. Soc.* **2004**, *126*, 5577.
(11) Lu, M.; Wei, Y.; Xu, B.; Cheung, C. F.-C.; Peng, Z.; Powell, D. *Angew. Chem. Int. Ed.* **2002**, *41* (9), 1566.
(12) Wei, Y.; Xu, B.; Barnes, C. L.; Peng, Z. *J. Am. Chem. Soc.* **2001**, *123*, 4083. (b) Xu, L.; Lu, M.; Xu, B.; Wei, Y.; Peng, Z. and Powell, D. R. *Angew. Chem., Int. Ed.* **2002**, *41*, 4129.
(13) Xu, B.; Wei, Y.; Barnes, C. L.; Peng, Z. *Angew. Chem. Int. Ed.* **2001**, *40*, 2290.

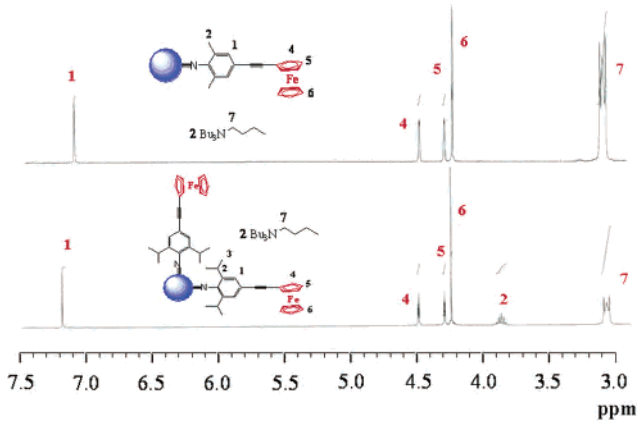

Figure 1. ^{1}H NMR spectra of hybrids **2a** and **2b**.

to ν(Mo−O_c−Mo) and ν(Mo−O_b−Mo), respectively. In the M═O stretching region of 900−1000 cm^{-1}, one strong band at 952 cm^{-1} and one sharp shoulder band at 975 cm^{-1} are observed. These two bands are assigned to ν(Mo−O_t) and ν(Mo−N), respectively. The ν(C≡C) stretching band appears at 2208 cm^{-1}. All these bands are observed in the spectrum of **2b** as well, with ±10 cm^{-1} shifts except for the ν(Mo−O_c−Mo) band, which has a −16 cm^{-1} shift. The relative intensity ratio of the ν(Mo−N) band over the ν(Mo−O_t) band, however, is noticeably higher in **2b** than that in **2a**, reflecting more Mo−N bonds in **2b**.

The structures of **2a** and **2b** were also studied by electrospray ionization mass spectrometry (ESI-MS). ESI-MS is becoming an important tool not only for the purpose of confirming the structure and assessing the purity of functionalized polyoxometalates, but also for gaining insights into the stability of these hybrid anions.[14] The mass spectrum of **2a** shows isotopic clusters centered at *m*/*z* 596.57 (100%), 1190.66 (19%), and 1434.10 (13%). These signals can be assigned to the cluster anion M^{2-} (M = $[Mo_6O_{18}NC_{10}H_8Fc]$, calculated *m*/*z* 595.4), $M^{2-} + H^+$ (calculated *m*/*z* 1191.8), and $M^{2-} + Bu_4N^+$ (calculated *m*/*z* 1433.3), respectively. Aside from these peaks, the mass spectrum of **2a** also shows signals at *m*/*z* 440.46 (12%) and 554.31 (12%). The former can be assigned to the parent $[Mo_6O_{19}]^{2-}$ cluster (calculated *m*/*z* 439.8), while the one at 554.31 is attributed to the anion in **1a** (calculated *m*/*z* 554.35). For hybrid **2b**, the M^{2-} (calculated *m*/*z* 807.0), $M^{2-} + H^+$ (calculated *m*/*z* 1615.0), and $M^{2-} + Bu_4N^+$ (calculated *m*/*z* 1856.4) peaks are also the dominant peaks, appearing at 807.88 (100%), 1617.98 (10%), and 1857.42 (6%), respectively, confirming the attachment of two ferrocenyl units.

The structure of **2a** is also confirmed by single-crystal X-ray diffraction. **2a** crystallizes in the triclinic space group $P\bar{1}$. As shown in Figure 2, the ferrocene and the hexamolybdate cluster are indeed bound together through a rigid rodlike organic bridge. The structure shows features typical of imido derivatives of hexamolybdates.[8−9,11] For example, the central oxygen atom inside the cluster cage is drawn significantly closer to the imido-bearing Mo atom (the bond

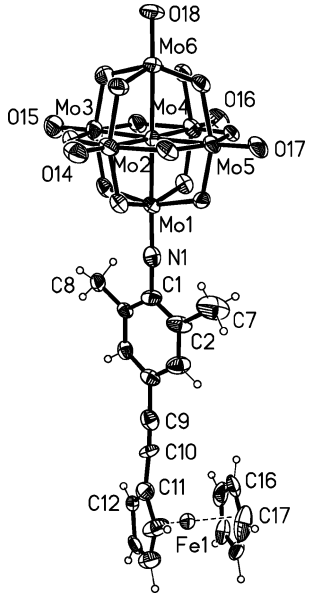

Figure 2. Anion structure of **2a**. The displacement ellipsoids were drawn at the 50% probability level. Selected bond lengths (Å) and bond angles (deg): Mo1−N1 1.731(8), Mo1−O1 2.205(5), Mo2−O14 1.691(6), Mo2−O1 2.323(5), Mo3−O15 1.680(6), Mo3−O1 2.338(4), Mo4−O16 1.685(6), Mo4−O1 2.336(5), Mo5−O17 1.682(5), Mo5−O1 2.329(4), Mo6−O18 1.676(6), Mo6−O1 2.356(5), N1−C1 1.405(10); Mo1−N1−C2 178.5(6).

length of Mo1−O1, compared to that of Mo6−O1, is shorter by 0.15 Å). The Mo−N bond shows triple bond character as reflected by the short Mo−N bond length (1.731(8) Å) and the linear Mo−N−C bond angle (178.5(6)°). The ferrocene unit displays the typical sandwich geometry with the two Cp rings in nearly eclipsed conformation. The average offset angle between the two Cp rings is only 6.8(9)°. The average Fe−C distances to the ethynyl Cp ligand and the bare Cp ligand are 2.035(9) and 2.010(10) Å, respectively, which are slightly shorter than the 2.050(2) Å found in $FeCp^*_2$ (Cp* = C_5Me_5),[15] and comparable to that in ferrocene itself (2.030 Å).[16] Significant variation between individual Fe−C distances is noted, particularly to the bare Cp ring (1.977(11)−2.046(9) Å, Δ = 0.069 Å). While most ferrocene derivatives show insignificant Fe−C distance variation, a similar large variation has been observed for a pentafluorophenyl-substituted ferrocene derivative.[17] The phenyl ring and the acetylene-bound Cp ring are significantly twisted as a large dihedral angle of 26.8(9)° is observed, indicating limited π-conjugation extending across the Cp ring and the phenyl ring.

Within the lattice, the hybrid anions pack in layers along the *c*-axis (Figure 3) with counterions filling the interlayer spaces. In each layer, the hybrid anions arrange in such a way that all ferrocenyl units point in the same direction. This direction is reversed at the adjacent layers. Within each layer, a two-dimensional network is formed through nonconven-

(14) Waters, T.; O'Hair, R. A.; Wedd, A. G. *J. Am. Chem. Soc.* **2003**, *125*, 3384. (b) Dablemont, C.; Proust, A.; Thouvenot, R.; Afonso, C.; Fournier, F.; Tabet, J.-C. *Inorg. Chem.* **2004**, *43*, 3514−3520.

(15) Freyburg, D. P.; Robbins, J. L.; Raymond, K. N.; Smart, J. C. *J. Am. Chem. Soc.* **1979**, *101*, 892.

(16) Seiler, P.; Dunitz, J. D. *Acta Crystallogr., Sect. B* **1979**, *B35*, 1068. (b) Takusagawa, F.; Koetzle, T. F. *Acta Crystallogr., Sect. B* **1979**, *B35*, 1074.

(17) Blanchard, M.; Hughes, R. P.; Concolino, T. E.; Rheingold, A. L. *Chem. Mater.* **2000**, *12*, 1604.

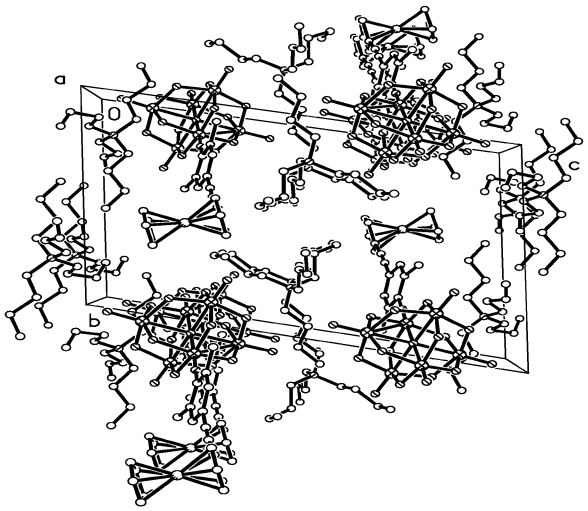

Figure 3. Packing drawing of **2a**.

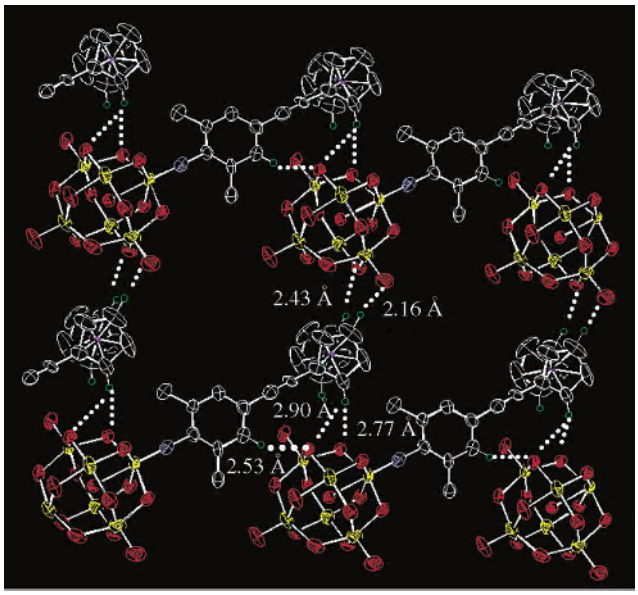

Figure 4. A two-dimensional network formed through multiple hydrogen bonding (most of the hydrogen atoms are omitted for clarity).

tional hydrogen bonding involving CH···O.[18] As shown in Figure 4, each ferrocenyl unit is flanked by two clusters and vice versa. Multiple hydrogen bonds exist between the closely approached clusters and the ferrocenyl moiety. The ferrocenyl unit appears to be slightly closer to one cluster than the other as the closest H···O distances to one cluster are 2.16 and 2.43 Å, while those to the other are 2.77 and 2.90 Å. There appear to be hydrogen bonds between μ_2-O of the cluster and aryl hydrogen as well (2.53 Å).

Electronic Properties. The electronic properties of **2a** and **2b** were studied by UV/vis absorption and fluorescence measurements. As shown in Figure 5, both **2a** and **2b** in acetonitrile show an intense absorption at 382 nm, which is assigned to the ligand-to-metal charge-transfer transition associated with the Mo−N π-bonding. The molar extinction coefficients at this particular wavelength are 3.39×10^4 and 5.60×10^4, respectively, for **2a** and **2b**. We have previously

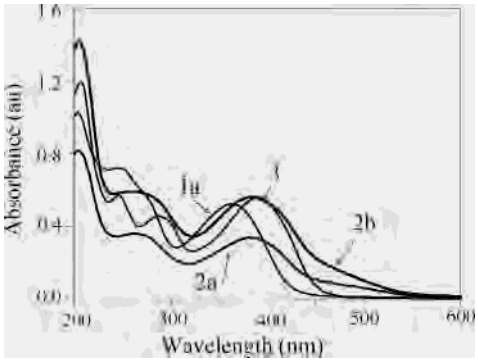

Figure 5. UV/vis absorption spectra of **1a**, **2a**, **2b**, and **3**.

reported a hybrid with a diphenylacetylene organic segment.[13] Its structure can be represented by replacing the ferrocenyl unit in **2a** with a *p*-methylphenyl group. Figure 5 also shows the spectrum of this hybrid, which is labeled as **3**, for comparison. It is noted that the maximum absorption wavelength of **3** is about 10 nm red shifted compared to those of **2a** and **2b**, presumably due to the more extended π-conjugation in **3** as the two phenyl rings in **3** are nearly planar.[13] At a longer wavelength range, a clear absorption tail extending beyond 550 nm is observed for both **2a** and **2b**. Considering the fact that both **1a** and ethynylferrocene, as well as hybrid **3**, exhibit no absorption in this range, the absorption tail is likely due to an intramolecular charge-transfer transition from the ferrocenyl unit to the cluster. As mentioned earlier, such a transition has also been observed in the (ferrocenylimido)hexamolybdate, $[(FcN)Mo_6O_{18}]^{2-}$, but as a much stronger and broader band centered at a much longer wavelength of 536 nm.[9] The Fe−Mo(1) distance in $[(FcN)Mo_6O_{18}]^{2-}$ is 4.78 Å, while the Fe−Mo(1) separation in **2a** is 11.29 Å. The charge- transfer resonance contribution to the ground state is thus expected to be much larger in $[(FcN)Mo_6O_{18}]^{2-}$ as compared to that in **2a** or **2b**, resulting in enhanced ground-state and diminished charge-separated-state polarization,[19] which in turn leads to a more pronounced charge-transfer band in $[(FcN)Mo_6O_{18}]^{2-}$. It is still remarkable though that clear charge-transfer bands are observed in **2a** and **2b** albeit there is an exceedingly large donor−acceptor separation distance of over 11 Å, which perhaps reflects the through-bond nature of the charge-transfer resonance made possible by the π-conjugated linker. Fluorescence studies show that hybrids **2a** and **2b** give no fluorescence emissions under excitation from 200 to 550 nm.

Electrochemistry. Figure 6 shows the cyclic voltammograms of a physical mixture of $[Bu_4N]_2[Mo_6O_{19}]$ with ferrocene and the covalently bonded hybrids **2a** and **2b**. Their redox potentials and peak currents are given in Table 1.

In the range −1.5 to +1.0 V (vs Ag/Ag^+), hybrid **2a** shows one reversible reduction wave at −0.831 V ($\Delta E = 0.26$ V) and one oxidation wave at 0.328 V ($\Delta E = 0.22$ V). **2b** also shows one reversible reduction wave, but at a higher potential of −1.055 V, and one oxidation wave at 0.331 V. Under the same conditions, the noncoupled parent $[Mo_6O_{19}]^{2-}$

(18) MacDonald, J. C.; Whitesides, G. M. *Chem. Rev.* **1994**, *94*, 2383.

(19) Rubtsov, I.; Kang, Y. K.; Redmore, N. P.; Allen, R. M.; Zheng, J.; Beratan, D. N.; Therien, M. J. *J. Am. Chem. Soc.* **2004**, *126*, 5022.

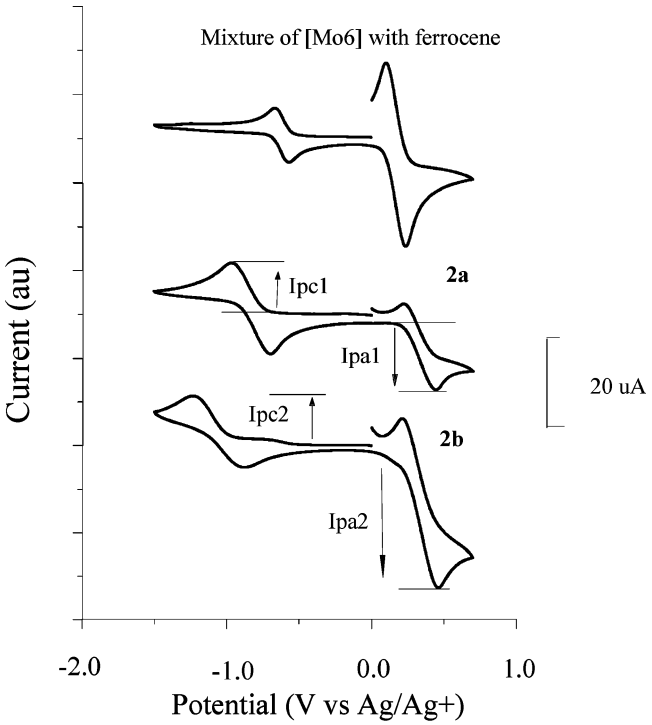

Figure 6. Cyclic voltammograms of a physical mixture of $[Bu_4N]_2[Mo_6O_{19}]$ with ferrocene, **2a**, and **2b**.

Table 1. Redox Potentials and Peak Currents of $[Mo_6O_{19}]^{2-}$, Ferrocene, **2a**, and **2b**[a]

compound	$E_{1/2}$,[b] V	E_{ox},[c] V	I_{pc}, μA	I_{pa}, μA
$Mo_6O_{19}^{2-}$	−0.620			
ferrocene		0.165		
2a	−0.831	0.328	12	16
2b	−1.055	0.331	12	33

[a] DMSO solution, 298 K, Pt working electrode, $[Bu_4N]PF_6$, supporting electrolyte, 100 mV s^{-1}. [b] $E_{1/2}$ vs Ag/Ag^+. [c] Edge value (irreversible oxidation).

cluster and ferrocene give one reversible reduction wave at −0.620 V and one oxidation wave at 0.165 V, respectively. The reduction process in **2a** and **2b** is thus associated with the cluster segment. The cathodically shifted reduction potential from the $[Mo_6O_{19}]^{2-}$ ion to **2a**, and further to **2b**, reflects the electron-donating nature of the imido ligand, which has been well documented.[8b] The oxidation wave in **2a** and **2b** is attributed to the ferrocenyl segment. The higher oxidation potential observed in **2a** and **2b** relative to that of ferrocene signals the electron-withdrawing nature of the linked cluster to the Cp ring.

While the ferrocenyl segment in **2a** and **2b** shows nearly identical oxidation potential, indicating negligible electronic interactions between the two vertically joined organic arms, their peak currents relative to that of the reduction process associated with the cluster anion are significantly different. On the basis of the Randle−Sevcik equation,[20] the peak current of a reversible redox process can be expressed as

$$I_p = kn^{3/2}AD^{1/2}CV^{1/2}$$

where k is a constant, n is the number of moles of electrons transferred per mole of electroactive species, A is the area of the electrode, D is the diffusion coefficient, C is the concentration of the electroactive species, and V is the scan rate.

For a given electroactive species, the parameters of k, A, D, C, and V are the same for both the reduction and oxidation processes. The ratio of I_{pa}/I_{pc} is thus related directly to the number of electrons involved in the oxidation and reduction process through the following equation:

$$I_{pa}/I_{pc} = (n_{pa}/n_{pc})^{3/2}$$

Here n_{pa} and n_{pc} are the number of electrons involved in the oxidation and reduction processes, respectively, per electroactive molecule.

Using the I_{pa} and I_{pc} values shown in Table 1, the n_{pa}/n_{pc} ratio of **2a** and **2b** is found to be 1.21 and 1.96, respectively. It is known that the reduction process of the $[Mo_6O_{19}]^{2-}$ anion at −0.620 V is a one-electron process. The above analysis indicates that the oxidation wave in **2a** is a one-electron process while that in **2b** is a two-electron process, confirming once again there are two ferrocenyl units attached to the cluster in **2b** and those two ferrocenyl units exhibit negligible electronic interactions.

Conclusions

Two new charge-transfer hybrids with one or two ferrocenyl units covalently attached to a hexamolybdate cluster through an extended π-conjugated bridge have been prepared using Pd-catalyzed coupling reactions on monoiodo- or diiodo-functionalized cluster substrates in over 60% yields. These hybrids have been characterized by ^{1}H NMR, FTIR, ESI-MS, and X-ray diffraction. The electronic spectra of these hybrids show a broad absorption tail extending beyond 550 nm, indicating the existence of a charge-transfer transition from the ferrocenyl donor to the cluster acceptor. The observation of the clear charge-transfer transition indicates the contribution of charge-transfer resonance to the ground state in both **2a** and **2b** even though the donor−acceptor separation distance of 11.29 Å is rather long, signaling a through-bond charge-transfer nature made possible by the organic π-conjugated bridge. Cyclic voltammetry studies reveal a one-electron oxidation wave and a one-electron reduction wave for the hybrid with one ferrocenyl unit. For the one with two ferrocenyl units, a lower reduction potential and a two-electron oxidation wave are observed, indicating negligible electronic interactions between the two ferrocenyl units.

Experimental Section

The syntheses of compounds **1a**[12a] and **1b**[12b] have been reported previously. All of the other chemicals were purchased either from Acros or from Aldrich and were used as received unless otherwise stated. The ^{1}H NMR spectra were collected on a Varian 400 MHz FT NMR spectrometer. Mass spectrometric experiments were conducted on a TSQ7000 triple-quadrupole mass spectrometer (ThermoFinnigan, San Jose, CA) with the API2 source and

(20) Bard, A. J.; Faulkner, L. R. *Electrochemical Methods: Fundamentals and Applications*; Wiley: New York, 2001.

Performance Pack. The heated inlet capillary was maintained at 250 °C. For ESI, the voltage on the stainless steel electrospray needle was between 2.5 and 4.5 kV for each sample and was adjusted to give a good ion signal with the current between 1 and 80 μA. Nitrogen sheath gas was provided at 80 psi. Samples were infused at a rate of 10 μL/min using a syringe pump (Harvard Apparatus, Holliston, MA). All samples were prepared immediately prior to use by dissolving a solid sample in HPLC-grade acetonitrile (Fisher Scientific, Fair Lawn, NJ). Samples were prepared in concentrations of 10−30 μM. The spectra acquired for each sample are an average of 150 individual scans or spectra.

A Hewlett-Packard 8452A diode array spectrophotometer was used to record the UV/vis absorption spectra. Fluorescence studies were performed on a Shimadzu P5301 fluorometer. Cyclic voltammetry (CV) studies were carried out in DMSO at room temperature under the protection of argon using a BAS Epsilon EC electrochemical station employing a 1 mm^2 Pt disk as the working electrode, a Ag/Ag^+ electrode (0.01 M $AgNO_3$) as the reference electrode, and a Pt wire as the counter electrode. $[Bu_4N]PF_6$ was the supporting electrolyte, and the scan rate was 100 mV s^{-1}.

Synthesis of Hybrid 2a. Triethylamine (0.27 mL) was added to the reaction mixture of **1a** (1.50 g, 0.95 mmol), ethynylferrocene (0.20 g, 0.95 mmol), $[PdCl_2(PPh_3)_2]$ (0.026 g, 0.038 mmol), and copper(I) iodide (0.014 g, 0.076 mmol) in DMF (anhydrous, 10 mL), and the resulting mixture was stirred at room temperature for 8 h under N_2. A 10 mL portion of water was then added to the mixture, followed by extraction with CH_2Cl_2. The organic layer was washed three times with water and dried with $MgSO_4$. After the solvent was stripped off, the resulting red powder was recrystallized from acetonitrile and dried in a vacuum oven at room temperature to give 1.10 g of **2a** as red crystals (1.10 g, 69.4%). The single crystals used for X-ray diffraction were obtained by slow diffusion of diethyl ether into a solution of **2a** in dichloromethane. ^{1}H NMR (400 MHz, CD_3CN, ppm): δ 7.14 (s, ArH, 2H), 4.48 (br, ArH, 2H), 4.29 (br, ArH, 2H), 4.23 (s, ArH, 5H), 3.07 (t, J = 8.4 Hz, NCH_2, 16H), 2.58 (s, (Ar)CH_3, 6H), 1.59 (tt, J = 7.6 and 8.4 Hz, CH_2, 16H), 1.34 (tq, J = 7.2 and 7.6 Hz, CH_2, 16H), 0.95 (t, J = 7.2 Hz, CH_3, 24H). UV/vis [MeCN; λ/nm (ϵ/M^{-1} cm^{-1})]: 205 (8.50×10^4), 260 (3.40×10^4), 382 (3.39×10^4). A red block-shaped crystal of dimensions 0.17 × 0.14 × 0.06 mm was selected for structural analysis. Summary of crystal structure data for **2a**: $C_{52}H_{89}FeMo_6N_3O_{18}$, M_r = 1675.75, triclinic, $P\bar{1}$, a = 11.587(2) Å, b = 13.574(2) Å, c = 20.629 (3) Å, α = 77.718(3)°, β = 77.659(4)°, γ = 88.614(4)°, V = 3096.3(8) $Å^3$, Z = 2, Z' = 1, T = 100(2) K, 15864 reflections measured, 15864 unique (R_{int} = 0.0000), R1 = 0.0692, wR2 = 0.2158, GOF 0.975. CCDC-239986 contains the supplementary crystallographic data for this paper. These data can be obtained free of charge via www.ccdc.cam.ac.uk/conts/retrieving.html (or from the Cambridge Crystallographic Data Centre, 12 Union Rd., Cambridge CB21EZ, U.K.; fax (+44)1223-336-033; e-mail deposit@ccdc.cam.ac.uk).

Synthesis of Hybrid 2b. Hybrid **2b** was synthesized using the same reaction and workup procedure as that of **2a** (73%). ^{1}H NMR (400 MHz, CD_3CN, ppm): δ 7.20 (s, ArH, 4H), 4.49 (t, J = 2.0 Hz, ArH, 4H), 4.29 (t, J = 2.0 Hz, ArH, 4H), 4.24 (s, ArH, 10H), 3.87 (m, (Ar)C*H*Me_2, 4H), 3.07 (t, J = 8.4 Hz, NCH_2, 16H), 1.59 (tt, J = 7.6 and 8.0 Hz, CH_2, 16H), 1.34 (tq, J = 7.2 and 7.6 Hz, CH_2,16H), 1.29 (d, J = 6.8 Hz, (Ar)CH*Me_2*, 24H), 0.95 (t, J = 7.2 Hz, CH_3, 24H). UV/vis [MeCN; λ/nm (ϵ/M^{-1} cm^{-1})]: 207 (1.47×10^5), 260 (5.50×10^4), 384 (5.60×10^4).

Acknowledgment. We gratefully acknowledge the support of this work by the National Science Foundation (DMR0134032) and the Office of Naval Research. We also thank Dr. Nathan D. Leigh at the University of Missouri−Columbia for the ESI-MS measurements.

IC049250X